Published in final edited form as:
J Proteome Res. 2012 December 7; 11(12): 5947–5958. doi:10.1021/pr300686k.

Assessment of Two Immunodepletion Methods: Off-Target Effects and Variations in Immunodepletion Efficiency May Confound Plasma Proteomics

Bhavinkumar B. Patel[†], **Carlos A. Barrero**[‡], **Alan Braverman**[§], **Phillip D. Kim**[†], **Kelly A. Jones**[†], **Dian Er Chen**[#], **Russell P. Bowler**[**], **Salim Merali**[‡], **Steven G. Kelsen**[§], and **Anthony T. Yeung**[*,†]

Developmental therapeutics Program, Fox Chase Cancer Center, Philadelphia, Pennsylvania 19111, Departments of Biochemistry and Medicine, Temple University School of Medicine Philadelphia, Pennsylvania 19140; National Jewish Health, Denver, CO 80206; and Sigma-Aldrich Biotechnology, Saint Louis, Missouri, 63103

Abstract

Immunodepletion of abundant plasma proteins increases the depth of proteome penetration by mass spectrometry. However, the nature and extent of immunodepletion and the effect of off-target depletion on the quantitative comparison of the residual proteins have not been critically addressed. We performed mass spectrometry label-free quantitation to determine which proteins were immunodepleted and by how much. Two immunodepletion resins were compared: Qproteome (Qiagen) which removes albumin+immunoglobulins and Seppro IgY14+SuperMix (Sigma-Aldrich) which removes 14 target proteins plus a number of unidentified proteins. Plasma collected by P100 proteomic plasma collection tubes (BD) from 20 human subjects was individually immunodepleted to minimize potential variability, prior to pooling. The abundant proteins were quantified better when using only albumin+immunoglobulins removal (Qproteome) while lower abundance proteins were evaluated better using exhaustive immunodepletion (Seppro IgY14+SuperMix). The latter resin removed at least 155 proteins, 38% of the plasma proteome in protein number and 94% of plasma protein in mass. The depth of immunodepletion likely accounts for the effectiveness of this resin in revealing low abundance proteins. However, the more profound immunodepletion achieved with the IgY14+SuperMix may lead to false-positive fold-changes between comparison groups if the reproducibility and efficiency of the depletion of a given protein is not considered.

Keywords

immunodepletion; Seppro; IgY; Qproteome; iTRAQ; EMMOL normalization; off-target

[*]To whom correspondence should be addressed: Anthony Yeung, PhD, Fox Chase Cancer Center, 333 Cottman Avenue, Philadelphia, PA 19111, Tel: +1-215-728-2488. FAX: +1-215- 728-3647. Anthony.Yeung@fccc.edu.
[†]Developmental therapeutics Program, Fox Chase Cancer Center, Philadelphia, PA 19111.
[‡]Departments of Biochemistry and
[§]Medicine, Temple University School of Medicine Philadelphia, PA 19140.
[**]National Jewish Health, Denver, CO 80206.
[#]Sigma-Aldrich Biotechnology, Saint Louis, MO, 63103

Conflicts of interests

Dr. Dian Er Chen who performed the immunodepletion steps was employed by Sigma-Aldrich that sells the IgY14+SuperMix column. Other authors declare no competing interest and no support by any company in connection with this work or future related work.

This article contains Supporting Information for Publication.

INTRODUCTION

The large dynamic range of protein concentration in plasma, i.e., nine orders of magnitude[1], has necessitated the removal of the higher abundance proteins to visualize the low abundance proteins. Immunodepletion of one or more high abundance proteins using antibody affinity immunoabsorption of specific antigens is one method used to accomplish this purpose. Initial application of immunodepletion to proteomics consisted of the depletion of serum albumin[2]. Subsequent methods, including the Qproteome (Qiagen) matrix, also remove immunoglobulins. Further generations of immunoaffinity columns, including the popular Multiple Affinity Removal System Columns (Agilent) and the ProteoPrep20 Immunodepletion Column (Sigma-Aldrich) remove several more proteins[3–5].

To accomplish depletion of a greater number of proteins, the SuperMix resin was created by Sigma-Aldrich by immunization of rabbits with the protein fraction that did not bind to an IgY14 column. In principal, the medium abundance, immunogenic proteins, now enriched, in this fraction induced antibodies for the SuperMix column. However, the targets of the SuperMix resin have never been fully identified and the ability of the Seppro IgY14+SuperMix column (Sigma-Aldrich) to allow quantitation of low abundance proteins is unstudied.

When a given protein is targeted for antibody-mediated removal, protein-protein interactions can lead to the removal of multiple proteins. The terms albuminome and depletome have been proposed to describe the proteins that are bound to albumin or other proteins during immunodepletion [6–9]. Estimations of the number of proteins that bind to albumin range from 24 to 67 depending on the methods used [8, 9]. A recent report performed an IgY14 column and a SuperMix column in tandem, compared their depleted proteomes and concluded that numerous proteins were immunodepleted by taking the IgY14 exhaustive immunodepletion to the next higher level of exhaustive immunodepletion[10]. In contrast, our report quantified the immunodepletion efficiencies of individual plasma proteins by a single-stage pre-mixed IgY14+SuperMix column.

Success of immunodepletion approaches has often been measured as the detection of low abundance proteins. However, the nature and extent of immunodepletion and the effect of off-target depletion on the quantitative comparison of the residual proteins have not been critically addressed. We performed mass spectrometry label-free quantitation to determine which proteins were immunodepleted and by how much. Two popular immunodepletion resins were compared: Qproteome (Qiagen) which removes albumin and immunoglobulins and Seppro IgY14+SuperMix (Sigma-Aldrich) which removes 14 target proteins plus a number of unidentified proteins. We found that the IgY14+SuperMix column depleted a substantial portion of the plasma proteome including 155 proteins many of which were previously identified as disease biomarkers. The degree and variability of depletion of such biomarkers can be an issue when comparing their expression levels between groups. Thus exhaustive immunodepletion may lead to false positive or false negative results if both the variability and efficiency of the immunodepletion and the off-target removal of individual proteins are not addressed.

Finally, we combined the data from these two proteomes to yield a continuous quantitative picture of human plasma with 5 logs of dynamic range. The abundant proteins were favored when using only albumin+immunoglobulins removal while lower abundance proteins were evaluated better using exhaustive immunodepletion.

MATERIALS AND METHODS

Study Samples

Plasma samples were collected from 20 subjects using the BD™ P100 Blood Collection Tubes that contained protease inhibitors, according to manufacturer's instructions. The subjects studied were Caucasian male ex-smokers enrolled in the NIH COPDGene® project, a large multi-center, genome-wide association study designed to elucidate the genetic basis for Chronic Obstructive Pulmonary Disease (COPD)[11–18]. The use of plasma from subjects in this study was incidental and resulted from a desire to use high quality samples in this analysis.

Study Design

The study design for each of the two immunodepletion methods is shown in Figure 1. The 20 subjects were divided into two study groups of 10 subjects each i.e., Groups 1 and 2. Individual samples taken from disease and control groups were not mixed. To provide technical replicates for the study, iTRAQ 4-plex methodology was used since it allows four replicate experiments to be performed for each immunodepletion method and has the advantage of avoiding LC-MS/MS under-sampling.

The Depletion of High-Abundance Proteins

Two methods of immunodepletion were used according to the manufacturer's protocols i.e., the Qproteome spin column approach (Qproteome albumin/IgG Depletion Kit, Qiagen, Carson City, CA) [19] and the Seppro IgY14+SuperMix[20] (Seppro Human IgY14 Human SuperMix LC5, catalog number SEP000-KT, Sigma-Aldrich Inc., St. Louis, MO). Researchers using immunodepletion have expressed concern over the possibility of run-to-run variations in the performance of immunodepletion chromatography. One way to prevent such potential variations from negatively impacting this study is to smooth the putative fluctuations by pooling the samples produced by ten chromatography runs. 100 microliter of plasma of each subject was individually immunodepleted by each method. Then aliquots of depleted plasma of 20 subjects were pooled as two groups of 10 each after quality analysis by SDS PAGE and quantitation.

iTRAQ Proteomics

The iTRAQ proteomic analysis procedures used in the current study have been described in detail previously[21]. From the Qproteome immunodepletion, 100 micrograms of the pooled immunodepleted plasma protein from Group 1 subjects was digested with trypsin and labeled with the iTRAQ 114 label and as a replicate by the iTRAQ 115 label. 100 micrograms of the pooled immunodepleted protein from Group 2 was labeled with the iTRAQ 116 label and as a replicate by the iTRAQ 117 label. These four samples were pooled into an iTRAQ peptide isoelectric focusing fractionation experiment [21–23] using the pH range 4.0–4.5 18 cm long region of a 24 cm IPG strip (pH 3.5–4.5 GE Healthcare) separating the peptides into 65 fractions as previously described in detail[21]. An identical approach was used for the Seppro IgY14+SuperMix immunodepletion flow through fraction. LC-MS/MS on an Applied Biosystems QSTAR XL qTOF mass spectrometer was performed on each IEF fraction as previously described in detail [24] including a second LC-MS/MS run for each sample using an exclusion list generated from the first LC-MS/MS run to obtain better peptide coverage. Peak lists were generated by the Mascot.dll script written by Matrix Science for the QSTAR instrument. Peptide charges +2 and +3, and monoisotopic. Enzyme was specified as trypsin. The peak lists were combined. Data processing of peptides based on 95% confidence for peptide assignment, with ion score >20 and at least one Bold Red by Mascot 2.2 software as described, allowing no trypsin missed

cleavage and no methionine oxidation when calculating the emPAI score. Carbamidomethylation (Cys) was set as fixed modification. The precursor ion m/z tolerance was set at 150 ppm; the product ion m/z tolerance at 0.5 Da. SwissProt Database Release 2010_09 containing 519348 sequence entries was used. The false discovery rate was <3.5 % at the peptide level as determined by Mascot using a randomized SwissProt database. To avoid the possibility of missing identification of low abundance proteins, the database was searched again allowing one trypsin missed cleavage and variable methionine oxidation.

Both IEF (e.g.: OFFGEL of Agilent) and strong cation exchange HPLC (IEX) chromatography can produce the hyper-fractionation desired to minimize signal contamination in an iTRAQ quantitation experiment. IEF was used. Peptides focus at three tight pH ranges[22]. The narrow pH range of 4.0–4.5 contains about 1/3 of the total peptides and thus is another fractionation step. Having less peptide in the LC-MS/MS minimizes the amount of contamination of each targeted peptide peak being quantified.

Informatics

To calculate the immunodepletion efficiency of a protein, its concentration in the depleted plasma sample and in the initial plasma sample must be compared. Since our focus is the Seppro IgY14+Super Mix column, the Qproteome-depleted plasma was used as a surrogate for the initial plasma sample. This allowed us to assess the effect of the Seppro IgY14+Super Mix column on the lower abundance proteins that are difficult to detect in crude plasma.

Although the four samples in an iTRAQ 4-plex experiment were intended to be identical in total peptide quantity, we sought to correct for variations in protein load caused by protein assay, trypsin digestion, pipetting, and the labeling-chemistry efficiency in each of the iTRAQ channels. We thus used our recently-reported method of iTRAQ data normalization for hyper-fractionated samples called EMMOL[21] (emPAI score × molecular weight normalization). emPAI is the exponentially modified Peptide Abundance Index. EMMOL uses mass spectrometry data to deduce the amounts of each protein in the four iTRAQ channels from the iTRAQ ratios. EMMOL normalization of the total protein quantity in each iTRAQ channel is guided by weighting towards the more abundant proteins where mass spectrometry measurements are more accurate for determining the relative values of total protein. In contrast, an iTRAQ normalization scheme that weighs all iTRAQ-labeled peptides equally regardless of protein abundance will suffer from the low accuracy of the identification and quantitation of low-abundance proteins. The peptides derived from low-abundance proteins are relatively low in intensity, producing iTRAQ reporter ions of low intensities. Moreover, fewer of the different peptides anticipated from the protein sequences will be observed by the mass spectrometer due to ion suppression by the higher abundance proteins and the threshold of sensitivity of the instrument.

Protein Quantitation

Key values included in Tables 1–4 are the iTRAQ reporter ratios, UniProt ID, Title, Gene Symbol, prot score, prot_mass, prot_matches, prot_cover, prot_pi, and emPAI.

EMMOL method of proteome normalization[21] was used to calculate the protein concentration of each protein in each pooled plasma sample. EMMOL was demonstrated to be valid by using defined *E. coli* lysate samples over a 20 fold range of protein quantities and over three logs of dynamic range of protein abundance[21].

EMMOL uses the relationship from equation 4 of Ishihama et al.[25]:

$$\text{Protein content (weight \%)} = (\text{emPAI} \times \text{Mr}) / \sum (\text{emPAI} \times \text{Mr}) \times 100$$

where Mr = molecular weight.

emPAI score is proportional to the fraction of observed peptides/theoretical peptides for a given protein (allowing no methionine oxidation and no missed trypsin cleavage). “emPAI × molecular weight” value is roughly proportional to the abundance of a protein.

Thus the EMMOL data processing workflow involves:

1. Calculate (emPAI × molecular weight) for each protein as its total in four iTRAQ channels
2. Normalize each protein to the sum of all proteins for the 4 iTRAQ channels, herein 180 μg protein (the total amount loaded into the 4 channels but any arbitrary total protein value such as the normal plasma protein concentration could have been used instead).
3. Use the iTRAQ ratios of each protein to calculate the μg of this protein in each iTRAQ channel
4. Sum the total protein of each iTRAQ channel
5. Normalize the four channels each to 45 μg of protein
6. Normalize each protein in each channel to the total protein concentration, determined by protein assay, for the immunodepleted plasma with respect to original plasma volume
7. Compare the corresponding concentrations from the two immunodepletion methods for each protein

Calculation of the Efficiencies of Immunodepletion of Individual Proteins in Two Immunodepletion Experiments

To calculate the immunodepletion efficiencies for removing albumin and immunoglobulins from plasma by the Qproteome method, the values of serum albumin before immunodepletion was stipulated as 44 mg/mL and immunoglobulins were 24 mg/mL. These are representative values from clinical test reports. After immunodepletion, the Qproteome depleted plasma had a protein concentration of 62.4 mg/mL when equated to the original plasma volume. The IgY14+SuperMix depleted plasma had a protein concentration of 7.4 mg/mL when equated to the original plasma volume. These values were used to normalize the measurements of individual protein quantities obtained from EMMOL calculations. The averaged results of the four iTRAQ channels are shown under the header “Average mg/mL in depleted plasma” in Tables 1–4. The ratio of this value for each protein from the IgY14+SuperMix column immunodepletion compared with the value from the Qproteome immunodepletion produces the values under the header “% immunodepletion”.

Construction of a Plasma Proteome from Two Immunodepletion Experiments

A subset of proteins was each quantified in both immunodepletion approaches. However, a given protein may be more abundant in the depleted proteome of one immunodepletion method than the other, resulting in better peptide statistics for identification and better iTRAQ quantitation accuracy. The better quality of these two results where available for each protein was used to construct a composite continuous proteome for further analysis.

Moreover, the comparison of the proteomes of the two immunodepletion methods (Tables 1–4) was used to identify the medium abundance proteins and the non-targeted proteins removed by the Seppro IgY14+SuperMix column.

RESULTS AND DISCUSSION

A comparison of the proteins in the pooled plasma samples immunodepleted by two procedures is shown in Tables 1–4. Supporting Information for Publication is the full display of all the tables that are partially presented herein plus the original Mascot output data of the Qproteome proteome and the Seppro IgY14+SuperMix proteome. Although the intended quantity of protein in each label reaction was 45 micrograms, EMMOL calculations suggested that the values of the total peptides for each iTRAQ channel during LC-MS/MS varied by as much as 20%. For the Qproteome experiments, iTRAQ 114, 115, 116, and 117 channels were 40.1, 41.7, 47.6, and 50.6 micrograms, respectively. For the Seppro IgY14+SuperMix experiments, iTRAQ 114, 115, 116, and 117 channels were 39.9, 43.9, 46.6, and 49.9 micrograms, respectively. A 20% bias in an iTRAQ channel would tend to complicate accurate determination of small fold-changes among proteins that differ in expression in two proteomes and confound proteomics pathway analysis. Hence, normalization based on the mass spectrometry measurements of the high abundance proteins tends to restore precision for the iTRAQ comparison.

The resulting proteome contained 412 proteins with quantitation, of which 120 were present in both immunodepletion samples

IgY14 Depletion

The Qproteome and the Seppro IgY14+SuperMix methods removed most of the albumin and the immunoglobulins according to SDS PAGE (data not shown) and the latter matrix removed many other proteins not visualized in SDS PAGE. The IgY14 was designed to remove human serum albumin, IgG, fibrinogen, transferrin, IgA, IgM, haptoglobin, alpha2-macroglubulin, alpha1-acid glycoprotein, alpha1-antitrypsin, apo A-I HDL, apo A-II, complement C3, and apo B. Table 1 illustrates their immunodepletion efficiencies.

SuperMix Depletion

A reasonable indication that a protein has been immunodepleted by the SuperMix resin is that its level has decreased by about 80–90 % after passing through the SuperMix resin. This arbitrary cutoff range seemed suitable for this dataset and revealed that the resin removed most of another 76 proteins (Table 2), including: complement factor B, antithrombin-III, inter-alpha-trypsin inhibitor heavy chain H1, H2, and H4; ceruloplasmin, complement C4-A, vitronectin, hemoglobin subunit alpha, beta and delta, plasma protease C1 inhibitor, prothrombin, angiotensinogen, vitamin D-binding protein, histidine-rich glycoprotein, and alpha-1B-glycoprotein. In all, most of the 20 top-abundance plasma proteins were depleted, but not eliminated, by IgY14+SuperMix column.

Off-target Protein Removal

Many abundant proteins in serum double as carrier proteins with high affinity binding but this phenomenon has only been studied for a few abundant proteins. The carrier role of serum albumin for small molecules[26] and proteins [9] is well known. Another example is alpha 2 macroglobulin, the most abundant globulin in the blood that is not an immunoglobulin, is an effective protease inhibitor, blocks fibrinolysis and is a known carrier of prostate-specific antigen PSA[27, 28]. However, it also binds to numerous growth factors and cytokines, such as platelet-derived growth factor, basic fibroblast growth factor, TGF-β, insulin, and IL-1β. Driven by affinity removal by the high-abundance carrier proteins, these

off-target depleted proteins shown in Table 3 were not seen in the highly enriched Seppro IgY14+SuperMix fraction in spite of their relatively ease of identification, with many peptides each, in the Qproteome fraction. Table 3 illustrates 65 proteins of this class. Mass spectrometry under-sampling is unlikely to explain their absence in the Seppro IgY14+SuperMix fraction; and we designate these as off-target removals. Other explanations are plausible, including the possibility that some of these proteins were exceptionally immunogenic in production of SuperMix matrix. In all, about 155 plasma proteins, 38% of the plasma proteome in protein number in this report and 94% of plasma protein in mass, were removed from the plasma by the Seppro IgY14+SuperMix resin.

Proteins made Visible by Immunodepletion by IgY14+SuperMix

276 proteins were visible only in the Seppro IgY14+SuperMix sample (Supporting Information for Publication and partially in Table 4). Most of these proteins are of low abundance in the plasma.

Continuous Plasma Proteome is best Constructed from Two Immunodepletion Approaches

In general, proteins depleted by the Seppro IgY14+SuperMix column were analyzed with better peptide coverage in the Qproteome method. The opposite is true for proteins enriched by the IgY14+SuperMix column. Using EMMOL normalization to calculate the approximate concentrations of each protein in the plasma and the availability of two immunodepletion results, we combined the two proteomes to form a continuous protein concentration range of 5 logs. For each protein that can be quantified in the proteome of each immunodepletion protocol, the value with higher confidence level, because of higher peptide coverage (emPAI), was selected. A portion of this proteome is presented in Table 4 and in whole in Supporting Information for Publication.

Why is Assessment of the On-target and Off-target Removed Proteins Important to Blood Biomarker Studies?

Immunodepletion can be conveniently performed once on a pool of plasma of cases and then once on a pool of the plasma of the controls. That approach is expedient but variation in the efficiencies of the immunodepletion process from run to run between cases and controls can increase the potential for false discovery. The performance of immunodepletion may vary in different laboratories depending on the composition of the immunodepletion matrix used, the chosen ratio of plasma volume to immunodepletion column capacity, and the age of the column. Our comparison reported the overall immunodepletion efficiency of the combined resin for each protein in the proteome. Thus a useful database that indicates which proteins are at risk for false positives is provided. Based on our quantitation of the immunodepletion efficiency of each individual protein, we hypothesize that those proteins which have the highest percentage immunodepletion are at the highest risk of being identified as false-positives in differential proteomic studies. For example, 98% removal of a protein in cases versus 96% removal in controls may suggest one fold change incorrectly in the residual proteins when the two groups were equal in the original plasma. However, the design of our study does not allow us to identify individual at-risk proteins as false positives or false negatives. Some of the removed off-target proteins can be relatively low abundance proteins. Thus variation in their detection or quantification in comparator groups may cause them to be misinterpreted as disease biomarkers. On the other hand, we noticed that proteins that have been depleted by less than 50% in the Seppro IgY14+SuperMix immunodepletion method still report protein fold-changes comparable to the Qproteome method that did not deplete those proteins.

In summary, the current study illustrates that caution needs to be exercised in experiments involving immunodepletion. Nonetheless, after proper accounting for off-target protein loss, immunodepletion proteomics by two methods can provide accurate comparison of both high-abundance and low-abundance proteins. One method should account for the highly-abundant proteins and a separate method should more exhaustively deplete the less-abundant proteins.

Supplementary Material

Refer to Web version on PubMed Central for supplementary material.

Acknowledgments

We thank Brian Searle for critical reading of this manuscript and Dr. Karen Kawarta, Sigma-Aldrich, for performing the immunodepletion procedures.

This work was partially supported by the National Institutes of Health (NIH) grant RC2 HL101713, the National Cancer Institute, Work Assignment #16 of N01-CN-43309, the Driskill Foundation, Institutional Core Grant P30CA06927, Tobacco Settlement Funds from the Commonwealth of Pennsylvania, the Pew Charitable Trust, and the Kresge Foundation.

The abbreviations used are

COPD	Chronic Obstructive Pulmonary Disease
iTRAQ	Isobaric Tag for Relative and Absolute Quantitation
IEF	Isoelectric Focusing
IPG	Immobilized Polyacrylamide Gel
EMMOL	emPAI-Molecular Weight method of proteome normalization

References

1. Anderson NL, Polanski M, Pieper R, Gatlin T, Tirumalai RS, Conrads TP, Veenstra TD, Adkins JN, Pounds JG, Fagan R, Lobley A. The human plasma proteome: a nonredundant list developed by combination of four separate sources. Mol Cell Proteomics. 2004; 3(4):311–26. [PubMed: 14718574]
2. Burgess-Cassler A, Johansen JJ, Kendrick N. Immunodepletion of albumin from human serum samples. Clinica chimica acta; international journal of clinical chemistry. 1989; 183(3):359–65.
3. Beer LA, Tang HY, Sriswasdi S, Barnhart KT, Speicher DW. Systematic discovery of ectopic pregnancy serum biomarkers using 3-D protein profiling coupled with label-free quantitation. Journal of proteome research. 2011; 10(3):1126–38. [PubMed: 21142075]
4. Maccarrone G, Milfay D, Birg I, Rosenhagen M, Holsboer F, Grimm R, Bailey J, Zolotarjova N, Turck CW. Mining the human cerebrospinal fluid proteome by immunodepletion and shotgun mass spectrometry. Electrophoresis. 2004; 25(14):2402–12. [PubMed: 15274023]
5. Shen Z, Want EJ, Chen W, Keating W, Nussbaumer W, Moore R, Gentle TM, Siuzdak G. Sepsis plasma protein profiling with immunodepletion, three-dimensional liquid chromatography tandem mass spectrometry, and spectrum counting. Journal of proteome research. 2006; 5(11):3154–60. [PubMed: 17081067]
6. Koutroukides TA, Guest PC, Leweke FM, Bailey DM, Rahmoune H, Bahn S, Martins-de-Souza D. Characterization of the human serum depletome by label-free shotgun proteomics. Journal of separation science. 2011; 34(13):1621–6. [PubMed: 21644252]
7. Smith MP, Wood SL, Zougman A, Ho JT, Peng J, Jackson D, Cairns DA, Lewington AJ, Selby PJ, Banks RE. A systematic analysis of the effects of increasing degrees of serum immunodepletion in

terms of depth of coverage and other key aspects in top-down and bottom-up proteomic analyses. Proteomics. 2011; 11(11):2222–35. [PubMed: 21548096]

8. Scumaci D, Gaspari M, Saccomanno M, Argiro G, Quaresima B, Faniello CM, Ricci P, Costanzo F, Cuda G. Assessment of an ad hoc procedure for isolation and characterization of human albuminome. Analytical biochemistry. 2011; 418(1):161–3. [PubMed: 21782783]
9. Gundry RL, Fu Q, Jelinek CA, Van Eyk JE, Cotter RJ. Investigation of an albumin-enriched fraction of human serum and its albuminome. Proteomics Clinical applications. 2007; 1(1):73–88. [PubMed: 20204147]
10. Juhasz P, Lynch M, Sethuraman M, Campbell J, Hines W, Paniagua M, Song L, Kulkarni M, Adourian A, Guo Y, Li X, Martin S, Gordon N. Semi-targeted plasma proteomics discovery workflow utilizing two-stage protein depletion and off-line LC-MALDI MS/MS. Journal of proteome research. 2011; 10(1):34–45. [PubMed: 20936781]
11. Foreman MG, Zhang L, Murphy J, Hansel NN, Make B, Hokanson JE, Washko G, Regan EA, Crapo JD, Silverman EK, DeMeo DL. Early-onset chronic obstructive pulmonary disease is associated with female sex, maternal factors, and African American race in the COPDGene Study. American journal of respiratory and critical care medicine. 2011; 184(4):414–20. [PubMed: 21562134]
12. Han MK, Kazerooni EA, Lynch DA, Liu LX, Murray S, Curtis JL, Criner GJ, Kim V, Bowler RP, Hanania NA, Anzueto AR, Make BJ, Hokanson JE, Crapo JD, Silverman EK, Martinez FJ, Washko GR. Chronic obstructive pulmonary disease exacerbations in the COPDGene study: associated radiologic phenotypes. Radiology. 2011; 261(1):274–82. [PubMed: 21788524]
13. Kim DK, Jacobson FL, Washko GR, Casaburi R, Make BJ, Crapo JD, Silverman EK, Hersh CP. Clinical and radiographic correlates of hypoxemia and oxygen therapy in the COPDGene study. Respiratory medicine. 2011; 105(8):1211–21. [PubMed: 21396809]
14. Kim V, Han MK, Vance GB, Make BJ, Newell JD, Hokanson JE, Hersh CP, Stinson D, Silverman EK, Criner GJ. The chronic bronchitic phenotype of COPD: an analysis of the COPDGene Study. Chest. 2011; 140(3):626–33. [PubMed: 21474571]
15. Rambod M, Porszasz J, Make BJ, Crapo JD, Casaburi R. Six-minute walk distance predictors, including CT scan measures, in the COPDGene cohort. Chest. 2012; 141(4):867–75. [PubMed: 21960696]
16. Regan EA, Hokanson JE, Murphy JR, Make B, Lynch DA, Beaty TH, Curran-Everett D, Silverman EK, Crapo JD. Genetic epidemiology of COPD (COPDGene) study design. COPD. 2010; 7(1):32–43. [PubMed: 20214461]
17. Wan ES, Hokanson JE, Murphy JR, Regan EA, Make BJ, Lynch DA, Crapo JD, Silverman EK. Clinical and radiographic predictors of GOLD-unclassified smokers in the COPDGene study. American journal of respiratory and critical care medicine. 2011; 184(1):57–63. [PubMed: 21493737]
18. Washko GR, Lynch DA, Matsuoka S, Ross JC, Umeoka S, Diaz A, Sciurba FC, Hunninghake GM, San Jose Estepar R, Silverman EK, Rosas IO, Hatabu H. Identification of early interstitial lung disease in smokers from the COPDGene Study. Academic radiology. 2010; 17(1):48–53. [PubMed: 19781963]
19. Geoui, T.; Urlaub, H.; Plessmann, U.; Porschewski, P. Extraction of proteins from formalin-fixed, paraffin-embedded tissue using the Qproteome extraction technique and preparation of tryptic peptides for liquid chromatography/mass spectrometry analysis. In: Ausubel, Frederick M., et al., editors. Current protocols in molecular biology. Vol. Chapter 10. 2010. p. 27p. 1-12.
20. Qian WJ, Kaleta DT, Petritis BO, Jiang H, Liu T, Zhang X, Mottaz HM, Varnum SM, Camp DG 2nd, Huang L, Fang X, Zhang WW, Smith RD. Enhanced detection of low abundance human plasma proteins using a tandem IgY12-SuperMix immunoaffinity separation strategy. Molecular & cellular proteomics: MCP. 2008; 7(10):1963–73.
21. Kim PD, Patel BB, Yeung AT. Isobaric Labeling and Data Normalization without Requiring Protein Quantitation. Journal of biomolecular techniques: JBT. 2012; 23(1):11–23. [PubMed: 22468137]
22. Lengqvist J, Uhlen K, Lehtio J. iTRAQ compatibility of peptide immobilized pH gradient isoelectric focusing. Proteomics. 2007; 7(11):1746–52. [PubMed: 17476709]

23. Eriksson H, Lengqvist J, Hedlund J, Uhlen K, Orre LM, Bjellqvist B, Persson B, Lehtio J, Jakobsson PJ. Quantitative membrane proteomics applying narrow range peptide isoelectric focusing for studies of small cell lung cancer resistance mechanisms. Proteomics. 2008; 8(15): 3008–18. [PubMed: 18654985]

24. Ke E, Patel BB, Liu T, Li XM, Haluszka O, Hoffman JP, Ehya H, Young NA, Watson JC, Weinberg DS, Nguyen MT, Cohen SJ, Meropol NJ, Litwin S, Tokar JL, Yeung AT. Proteomic analyses of pancreatic cyst fluids. Pancreas. 2009; 38(2):e33–42. [PubMed: 19136908]

25. Ishihama Y, Oda Y, Tabata T, Sato T, Nagasu T, Rappsilber J, Mann M. Exponentially modified protein abundance index (emPAI) for estimation of absolute protein amount in proteomics by the number of sequenced peptides per protein. Mol Cell Proteomics. 2005; 4(9):1265–72. [PubMed: 15958392]

26. Fanali G, di Masi A, Trezza V, Marino M, Fasano M, Ascenzi P. Human serum albumin: from bench to bedside. Molecular aspects of medicine. 2012; 33(3):209–90. [PubMed: 22230555]

27. Lin VK, Wang SY, Boetticher NC, Vazquez DV, Saboorian H, McConnell JD, Roehrborn CG. Alpha(2) macroglobulin, a PSA binding protein, is expressed in human prostate stroma. The Prostate. 2005; 63(3):299–308. [PubMed: 15611997]

28. Zhang WM, Finne P, Leinonen J, Salo J, Stenman UH. Determination of prostate-specific antigen complexed to alpha(2)-macroglobulin in serum increases the specificity of free to total PSA for prostate cancer. Urology. 2000; 56(2):267–72. [PubMed: 10925092]

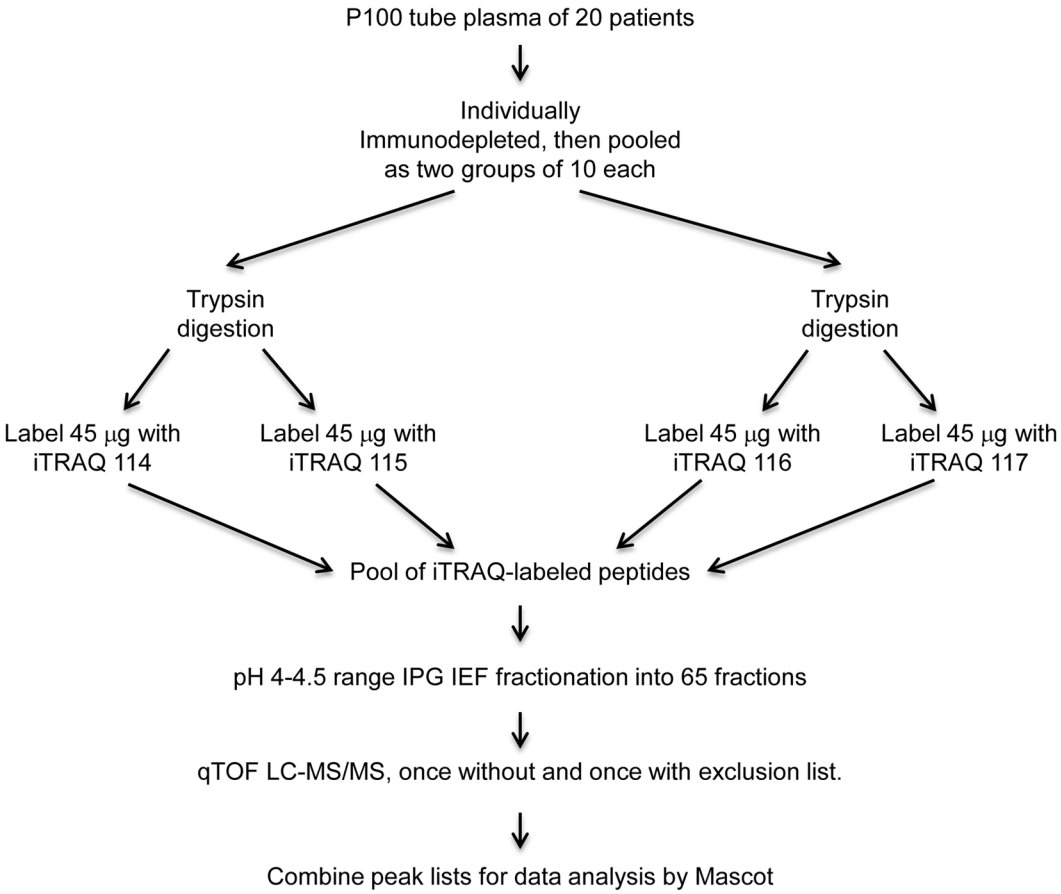

Figure 1.
Work flow of an immunodepletion evaluation experiment. The process was done once for the Qproteome method and once for the Seppro IgY14+SuperMix method.

J Proteome Res. Author manuscript; available in PMC 2013 December 07.

Table 1

Immunodepletion Efficiencies of the Targets of Qproteome and IgY14+SuperMix column

Immuno-depletion method	Title	Gene Symbol	prot_score	prot_mass	prot_matches	prot_cover	emPAI	Average mg/mL in depleted plasma	% immunodepletion
Qproteome	Serum albumin	ALB	4726	80107	236	39.2	2.71	1.17	97
Seppro	Serum albumin	ALB	3083	80107	137	38.4	2.24	0.09	99
Qproteome	Ig gamma-1 chain C region	IGHG1	8609	40775	409	39.4	2.43	0.58	93
Seppro	Ig gamma-1 chain C region	IGHG1	464	40775	28	10.3	0.42	0.01	99
Qproteome	Ig alpha-1 chain C region	IGHA1	6711	40503	264	25.8	1.89	0.42	93
Seppro	Ig alpha-1 chain C region	IGHA1	936	40503	43	22.4	1.03	0.02	96
Qproteome	Ig kappa chain C region	IGKC	6260	13070	168	69.8	3.84	0.29	93
Seppro	Ig kappa chain C region	IGKC	2458	13070	61	53.8	1.86	0.01	96
Qproteome	Ig mu chain C region	IGHM	5726	53274	209	40.7	2.38	0.72	93
Seppro	Ig mu chain C region	IGHM	4036	53274	196	44	2.87	0.08	87
Qproteome	Immunoglobulin J chain	IGJ	304	17049	8	7.5	0.5	0.05	93
Seppro	Immunoglobulin J chain	IGJ	174	19984	5	11.9	0.7	0.01	80
Qproteome	Complement C3	C3	29308	204997	1046	53.1	3.61	4.13	
Seppro	Complement C3	C3	1321	204997	51	13.1	0.31	0.03	99
Qproteome	Serotransferrin	TF	18294	87782	961	55.7	8.3	4.08	
Seppro	Serotransferrin	TF	1458	87782	64	27.9	1.1	0.05	98
Qproteome	Haptoglobin-related protein	HPR	7464	43675	334	30.7	3.4	0.82	
Seppro	Haptoglobin-related protein	HPR	875	43697	36	20.4	1.27	0.03	97
Qproteome	Haptoglobin	HP	10951	51048	620	47.3	6.74	1.90	
Seppro	Haptoglobin	HP	1523	51048	83	31.3	2.82	0.08	97
Qproteome	Apolipoprotein A-I	APOA1	24599	34073	1192	76.4	58.75	11.12	
Seppro	Apolipoprotein A-I	APOA1	11090	34073	532	77.5	34.37	0.62	95
Qproteome	Apolipoprotein A-II	APOA2	3135	12867	334	74	17.91	1.29	
Seppro	Apolipoprotein A-II	APOA2	508	12867	86	74	10.08	0.07	95
Qproteome	Alpha-1-acid glycoprotein 1	ORM1	3162	25886	150	48.3	4.19	0.61	
Seppro	Glial fibrillary acidic protein	ORM1	4211	25886	214	46.8	3.52	0.05	92

Immuno-depletion method	Title	Gene Symbol	prot_score	prot_mass	prot_matches	prot_cover	emPAI	Average mg/mL in depleted plasma	% immunodepletion
Qproteome	Alpha-1-acid glycoprotein 2	ORM2	1418	25890	95	31.3	2.44	0.35	
Seppro	Alpha-1-acid glycoprotein 2	ORM2	2546	25890	156	29.9	2.44	0.03	91
Qproteome	Alpha-2-macroglobulin	A2M	19430	177570	838	46	3.2	3.18	
Seppro	Alpha-2-macroglobulin	A2M	36377	177584	1446	53.4	4.96	0.48	84
Qproteome	Fibrinogen gamma chain	FGG	4757	57150	302	33.6	3.55	1.12	
Seppro	Fibrinogen gamma chain	FGG	4348	57150	283	48.1	4.85	0.15	84
Qproteome	Fibrinogen alpha chain	FGA	12367	101996	656	36.5	3.01	1.69	
Seppro	Fibrinogen alpha chain	FGA	13296	101996	690	42.6	5.36	0.30	79
Qproteome	Apolipoprotein B-100	APOB	13207	568255	471	25.2	0.91	2.90	
Seppro	Apolipoprotein B-100	APOB	31350	568096	1259	48.3	3.12	0.97	66

J Proteome Res. Author manuscript; available in PMC 2013 December 07.

Table 2

Immunodepletion Efficiencies of the 76 Putative Targets of Seppro SuperMix Resin

Immuno-depletion method	Title	Gene Symbol	prot_score	prot_mass	prot_matches	prot_cover	emPAI	Average mg/mL in depleted plasma	% immunodepletion
Qproteome	Complement factor B	CFB	2265	94629	110	21.6	1.32	0.698	
Seppro	Complement factor B	CFB	102	94629	2	1.8	0.04	0.002	100
Qproteome	Inter-alpha-trypsin inhibitor heavy chain H4	ITIH4	2298	109541	95	24.5	0.94	0.576	
Seppro	Inter-alpha-trypsin inhibitor heavy chain H4	ITIH4	51	109573	3	1.8	0.07	0.004	100
Qproteome	Inter-alpha-trypsin inhibitor heavy chain H2	ITIH2	1671	116337	55	15	0.55	0.357	
Seppro	Inter-alpha-trypsin inhibitor heavy chain H2	ITIH2	198	116364	5	2.3	0.03	0.002	100
Qproteome	Complement C4-A	C4A	4364	205487	181	24.2	1.03	1.178	
Seppro	Complement C4-A	C4A	168	205487	8	2.5	0.07	0.008	100
Qproteome	Antithrombin-III	SERPINC1	5520	58501	167	46.3	2.43	0.794	
Seppro	Antithrombin-III	SERPINC1	160	58501	4	5	0.13	0.004	100
Qproteome	Ceruloplasmin	CP	3498	132638	124	25.1	0.93	0.687	
Seppro	Ceruloplasmin	CP	74	132638	2	2.1	0.06	0.004	99
Qproteome	Vitronectin	VTN	1661	58096	47	20.7	0.86	0.281	
Seppro	Vitronectin	VTN	210	58096	4	3.1	0.06	0.002	99
Qproteome	Hemoglobin subunit alpha	HBA1	945	17034	37	35.2	2.43	0.231	
Seppro	Hemoglobin subunit alpha	HBA1	55	17034	2	8.5	0.23	0.002	99
Qproteome	Plasma protease C1 inhibitor	SERPING1	2382	59671	105	23.8	1.33	0.444	
Seppro	Plasma protease C1 inhibitor	SERPING1	124	59671	3	5.4	0.13	0.004	99
Qproteome	Vitamin D-binding protein	GC	1757	61010	83	23.2	1.03	0.351	
Seppro	Vitamin D-binding protein	GC	112	61010	3	6.3	0.19	0.006	99
Qproteome	Prothrombin	F2	1017	75798	28	12.5	0.4	0.169	
Seppro	Prothrombin	F2	49	75798	2	1.6	0.05	0.002	99
Qproteome	Angiotensinogen	AGT	977	56576	42	13.2	0.47	0.149	

Immuno-depletion method	Title	Gene Symbol	prot_score	prot_mass	prot_matches	prot_cover	emPAI	Average mg/mL in depleted plasma	% immunodepletion
Seppro	Angiotensinogen	AGT	278	56576	9	2.7	0.07	0.002	99
Qproteome	Inter-alpha-trypsin inhibitor heavy chain H1	ITIH1	2049	108699	55	13.4	0.4	0.242	
Seppro	Inter-alpha-trypsin inhibitor heavy chain H1	ITIH1	179	108699	5	4.2	0.07	0.004	99
Qproteome	Hemoglobin subunit beta	HBB	2335	17832	71	67.3	7.62	0.761	
Seppro	Hemoglobin subunit beta	HBB	629	17832	15	44.9	1.66	0.016	98
Qproteome	Histidine-rich glycoprotein	HRG	945	63825	36	17.9	0.57	0.203	
Seppro	Histidine-rich glycoprotein	HRG	60	63825	4	5	0.12	0.004	98
Qproteome	Alpha-1B-glycoprotein	A1BG	249	56538	24	9.5	0.21	0.066	
Seppro	Alpha-1B-glycoprotein	A1BG	38	56538	3	2	0.07	0.002	98
Qproteome	Hemoglobin subunit delta	HBD	1079	17889	42	50.3	2.94	0.294	
Seppro	Hemoglobin subunit delta	HBD	87	17889	8	32	0.8	0.008	98
Qproteome	Afamin	AFM	1139	78456	40	20.7	0.59	0.259	
Seppro	Afamin	AFM	775	78456	31	8.2	0.2	0.008	97
Qproteome	Complement component C7	C7	200	103711	5	3	0.07	0.039	
Seppro	Complement component C7	C7	219	103711	5	1.8	0.04	0.002	96
Qproteome	Alpha-1-antitrypsin	SERPINA1	16719	51922	799	64.6	8.86	2.550	
Seppro	Alpha-1-antitrypsin	SERPINA1	4261	51922	220	53.1	4.66	0.129	96
Qproteome	C4b-binding protein alpha chain	C4BPA	770	74086	23	8.9	0.41	0.169	
Seppro	C4b-binding protein alpha chain	C4BPA	395	74086	9	3.9	0.16	0.006	96
Qproteome	C4b-binding protein beta chain	C4BPB	77	32046	4	4	0.25	0.045	
Seppro	C4b-binding protein beta chain	C4BPB	51	32046	2	4	0.12	0.002	96
Qproteome	Dermcidin	DCD	56	12976	2	10	0.3	0.022	
Seppro	Dermcidin	DCD	77	12976	2	10	0.3	0.002	95
Qproteome	Kinesin-like protein KIF21B	KIF21B	77	199879	30	1	0.04	0.045	
Seppro	Kinesin-like protein KIF21B	KIF21B	104	199879	49	1	0.02	0.002	95
Qproteome	Apolipoprotein C-III	APOC3	1489	11854	56	55.6	6.52	0.437	
Seppro	Apolipoprotein C-III	APOC3	1199	11854	49	53.5	3.23	0.021	95

Immuno-depletion method	Title	Gene Symbol	prot_score	prot_mass	prot_matches	prot_cover	emPAI	Average mg/mL in depleted plasma	% immunodepletion
Qproteome	Complement C1q subcomponent subunit B	C1QB	238	28976	7	5.5	0.28	0.045	
Seppro	Complement C1q subcomponent subunit B	C1QB	276	29238	10	5.5	0.13	0.002	95
Qproteome	Heparin cofactor 2	SERPIND1	917	62105	29	18.4	0.5	0.174	
Seppro	Heparin cofactor 2	SERPIND1	292	62105	10	9.6	0.26	0.009	94
Qproteome	Ficolin-2	FCN2	152	36885	7	9.6	0.34	0.070	
Seppro	Ficolin-2	FCN2	147	36885	8	6.7	0.21	0.004	94
Qproteome	Interleukin-12 receptor beta-1 chain	IL12RB1	34	77456	6	2.3	0.05	0.022	
Seppro	Interleukin-12 receptor subunit beta-1	IL12RB1	36	77456	12	0.9	0.05	0.002	94
Qproteome	Serum amyloid A-4 protein	SAA4	355	16007	12	26.2	0.92	0.082	
Seppro	Serum amyloid A-4 protein	SAA4	250	16004	7	8.5	0.55	0.005	94
Qproteome	Phospholipid transfer protein	PLTP	182	57526	5	8.1	0.29	0.093	
Seppro	Phospholipid transfer protein	PLTP	381	57526	17	5.3	0.21	0.007	94
Qproteome	Complement factor I	CFI	306	74412	12	9.3	0.21	0.088	
Seppro	Complement factor I	CFI	154	74412	14	4.6	0.16	0.006	93
Qproteome	Tripartite motif-containing protein 37	TRIM37	46	116552	2	0.7	0.03	0.020	
Seppro	E3 ubiquitin-protein ligase TRIM37	TRIM37	70	116552	6	1.7	0.03	0.002	93
Qproteome	Complement component C9	C9	759	70091	29	8.4	0.36	0.140	
Seppro	Complement component C9	C9	337	70091	16	8.9	0.29	0.011	93
Qproteome	R3H domain-containing protein 1	R3HDM1	63	129519	2	0.6	0.03	0.022	
Seppro	R3H domain-containing protein 1	R3HDM1	54	129519	2	0.6	0.03	0.002	93
Qproteome	Complement C1s subcomponent	C1S	794	83650	29	14.2	0.54	0.251	
Seppro	Complement C1s subcomponent	C1S	766	83650	39	13.7	0.48	0.022	91
Qproteome	Apolipoprotein C-I	APOC1	627	10767	46	32.5	3.85	0.232	
Seppro	Apolipoprotein C-I	APOC1	373	10767	23	32.5	3.85	0.022	91
Qproteome	Alpha-1-antichymotrypsin	SERPINA3	4424	51682	158	38.3	1.65	0.475	
Seppro	Alpha-1-antichymotrypsin	SERPINA3	2975	51682	114	40.4	2.27	0.062	90

J Proteome Res. Author manuscript; available in PMC 2013 December 07.

Immuno-depletion method	Title	Gene Symbol	prot_score	prot_mass	prot_matches	prot_cover	emPAI	Average mg/mL in depleted plasma	% immunodepletion
Qproteome	Apolipoprotein C-II	APOC2	247	12285	13	45.5	2.05	0.142	
Seppro	Apolipoprotein C-II	APOC2	313	12285	12	57.4	2.05	0.014	90
Qproteome	UPF0505 protein C16orf62	C16orf62	32	120515	3	2.1	0.03	0.020	
Seppro	UPF0505 protein C16orf62	C16orf62	82	120515	4	2.1	0.03	0.002	90
Qproteome	Obscurin	OBSCN	217	928336	71	0.3	0.01	0.051	
Seppro	Obscurin	OBSCN	87	928336	34	0.6	0.01	0.005	90
Qproteome	Apolipoprotein D	APOD	147	23276	9	10.1	0.35	0.045	
Seppro	Apolipoprotein D	APOD	128	23276	5	10.1	0.35	0.004	90
Qproteome	Complement C1q subcomponent subunit C	C1QC	155	27859	3	7.3	0.14	0.022	
Seppro	Complement C1q subcomponent subunit C	C1QC	174	27859	3	7.3	0.14	0.002	90
Qproteome	A disintegrin and metalloproteinase with thrombospondin motifs 12	ADAMTS12	37	196369	8	0.9	0.02	0.022	
Seppro	A disintegrin and metalloproteinase with thrombospondin motifs 12	ADAMTS12	33	196355	6	0.9	0.02	0.002	89
Qproteome	Phosphatidylinositol-4,5-bisphosphate 3-kinase catalytic subunit beta isoform	PIK3CB	61	135868	26	1.2	0.03	0.023	
Seppro	Phosphatidylinositol-4,5-bisphosphate 3-kinase catalytic subunit beta isoform	PIK3CB	74	135868	25	0.7	0.03	0.002	89
Qproteome	Uncharacterized protein C2orf77	C2orf77	47	77323	3	1.1	0.05	0.022	
Seppro	Uncharacterized protein C2orf77	C2orf77	100	77323	22	1.1	0.05	0.002	89
Qproteome	Vacuolar fusion protein MON1homolog A	MON1A	52	64884	8	1.4	0.06	0.022	
Seppro	Vacuolar fusion protein MON1homolog A	MON1A	62	64884	9	1.4	0.06	0.002	89
Qproteome	T-complex protein 1 subunit zeta-2	CCT6B	127	65072	61	1.5	0.06	0.021	
Seppro	T-complex protein 1 subunit zeta-2	CCT6B	42	65072	23	2.8	0.06	0.002	88
Qproteome	ATP-binding cassette sub-family B member 9	ABCB9	126	88768	7	0.9	0.04	0.020	

Immuno-depletion method	Title	Gene Symbol	prot_score	prot_mass	prot_matches	prot_cover	emPAI	Average mg/mL in depleted plasma	% immunodepletion
Seppro	ATP-binding cassette sub-family B member 9	ABCB9	232	88768	17	0.9	0.04	0.002	88
Qproteome	Keratin, type I cytoskeletal 9	KRT9	221	66211	13	7.7	0.24	0.087	
Seppro	Keratin, type I cytoskeletal 9	KRT9	138	66146	13	5.8	0.24	0.008	88
Qproteome	Apolipoprotein L1	APOL1	573	47751	16	9.5	0.46	0.123	
Seppro	Apolipoprotein L1	APOL1	517	47751	25	11.6	0.57	0.015	87
Qproteome	Protein AMBP	AMBP	934	42624	36	25	0.52	0.125	
Seppro	Protein AMBP	AMBP	1308	42624	37	25	0.66	0.015	87
Qproteome	Fibronectin	FN1	1774	277418	49	7.4	0.17	0.261	
Seppro	Fibronectin	FN1	1648	277437	44	6.7	0.19	0.029	86
Qproteome	Hyaluronan-binding protein 2	HABP2	95	70504	2	1.6	0.11	0.043	
Seppro	Hyaluronan-binding protein 2	HABP2	349	70504	12	3.8	0.17	0.006	86
Qproteome	Complement-activating component of Ra-reactive factor	MASP1	161	86325	8	2.7	0.09	0.043	
Seppro	Mannan-binding lectin serine protease 1	MASP1	485	86325	20	2.7	0.13	0.006	86
Qproteome	Isocitrate dehydrogenase [NAD]subunit alpha, mitochondrial	IDH3A	131	43625	12	2.7	0.09	0.022	
Seppro	Isocitrate dehydrogenase [NAD]subunit alpha, mitochondrial	IDH3A	52	43625	3	2.7	0.18	0.004	84
Qproteome	Keratin, type I cytoskeletal 10	KRT10	728	63161	21	14.4	0.41	0.144	
Seppro	Keratin, type I cytoskeletal 10	KRT10	840	62478	29	17	0.68	0.023	84
Qproteome	Apolipoprotein E	APOE	1982	38263	45	41.3	2.71	0.579	
Seppro	Apolipoprotein E	APOE	2852	38263	100	46.1	5.5	0.113	83
Qproteome	Gelsolin	GSN	695	92672	16	11.8	0.22	0.114	
Seppro	Gelsolin	GSN	808	92672	24	13.9	0.37	0.019	83
Qproteome	CD5 antigen-like	CD5L	88	42052	2	4	0.09	0.022	
Seppro	CD5 antigen-like	CD5L	110	42052	4	6.1	0.19	0.004	82
Qproteome	Keratin, type II cytoskeletal 2epidermal	KRT2	359	71298	12	7.5	0.23	0.092	

Immuno-depletion method	Title	Gene Symbol	prot_score	prot_mass	prot_matches	prot_cover	emPAI	Average mg/mL in depleted plasma	% immunodepletion
Seppro	Keratin, type II cytoskeletal 2epidermal	KRT2	362	70866	18	11.7	0.43	0.016	80
Qproteome	Hypoxia up-regulated protein 1	HYOU1	99	122734	2	1.9	0.03	0.021	
Seppro	Hypoxia up-regulated protein 1	HYOU1	392	122734	13	6	0.09	0.006	80
Qproteome	Corticosteroid-binding globulin	SERPINA6	259	47877	9	7.2	0.25	0.067	
Seppro	Corticosteroid-binding globulin	SERPINA6	1344	47877	42	12.8	0.57	0.015	79
Qproteome	Inter-alpha-trypsin inhibitor heavy chain H3	ITIH3	262	108718	7	4	0.14	0.085	
Seppro	Inter-alpha-trypsin inhibitor heavy chain H3	ITIH3	513	108718	16	12	0.31	0.018	79
	Prostaglandin-H2 D-isomerase	PTGDS	139	22829	3	8.9	0.17	0.022	
Seppro	Prostaglandin-H2 D-isomerase	PTGDS	248	22829	15	12.6	0.36	0.004	79
Qproteome	L-lactate dehydrogenase B chain	LDHB	55	40791	2	7.5	0.19	0.043	
Seppro	L-lactate dehydrogenase B chain	LDHB	445	40791	11	12.3	0.42	0.009	79
Qproteome	Keratin, type II cytoskeletal 1	KRT1	380	70184	23	13.5	0.51	0.197	
Seppro	Keratin, type II cytoskeletal 1	KRT1	846	70349	40	19.9	1.16	0.043	78
Qproteome	Selenoprotein P	SEPP1	163	48016	8	8.1	0.25	0.067	
Seppro	Selenoprotein P	SEPP1	536	48016	25	16	0.57	0.015	77
Qproteome	Cystatin-C	CST3	125	17170	2	11	0.23	0.022	
Seppro	Cystatin-C	CST3	379	17170	10	18.5	0.5	0.005	77
Qproteome	Transthyretin	TTR	2397	17288	141	57.1	4.03	0.390	
Seppro	Transthyretin	TTR	2970	17288	191	73.5	8.21	0.078	76
Qproteome	Cartilage oligomeric matrix protein	COMP	131	88457	2	2.6	0.04	0.020	
Seppro	Cartilage oligomeric matrix protein	COMP	482	88457	9	5.8	0.13	0.006	76
Qproteome	Coagulation factor XIII A chain	F13A1	195	89348	8	6.1	0.13	0.065	
Seppro	Coagulation factor XIII A chain	F13A1	697	89348	22	10.5	0.28	0.014	76
Qproteome	Plasma serine protease inhibitor	SERPINA5	90	49389	4	5.9	0.16	0.044	
Seppro	Plasma serine protease inhibitor	SERPINA5	221	49389	10	11.1	0.34	0.009	75
Qproteome	Monocyte differentiation antigen CD14	CD14	162	42119	4	7.2	0.19	0.045	

Immuno-depletion method	Title	Gene Symbol	prot_score	prot_mass	prot_matches	prot_cover	emPAI	Average mg/mL in depleted plasma	% immunodepletion
Seppro	Monocyte differentiation antigen CD14	CD14	581	42119	21	14.7	0.53	0.012	75
Qproteome	Coagulation factor V	F5	249	271099	9	2.1	0.06	0.091	
Seppro	Coagulation factor V	F5	809	271099	33	5.5	0.16	0.023	74
Qproteome	Serum paraoxonase/arylesterase 1	PON1	1071	42921	25	18	0.29	0.070	
Seppro	Serum paraoxonase/arylesterase 1	PON1	1409	42921	59	27	0.95	0.022	74

J Proteome Res. Author manuscript; available in PMC 2013 December 07.

Table 3

65 Proteins Putatively Absorbed by Protein-protein Interactions on Seppro IgY14+SuperMix Column

Immuno-depletion method	Title	Gene Symbol	prot_score	prot_mass	prot_matches	prot_cover	emPAI	Average mg/mL in depleted plasma
Qproteome	Hemopexin	HPX	3086	55555	219	32.3	2.02	0.628
Qproteome	Phosphatidylinositol-4-phosphate 3-kinase C2domain-containing gamma polypeptide	PIK3C2G	106	182657	102	1.3	0.04	0.041
Qproteome	Centrosomal protein of 164 kDa	CEP164	94	179858	78	0.4	0.02	0.020
Qproteome	Kinesin-like protein KIF16B	KIF16B	41	169204	77	1.5	0.02	0.019
Qproteome	Alpha-2-HS-glycoprotein	AHSG	557	42548	76	19.1	0.97	0.232
Qproteome	Dynein heavy chain 17, axonemal	DNAH17	214	563266	74	0.2	0.01	0.031
Qproteome	Complement factor H	CFH	834	155353	57	11.2	0.26	0.225
Qproteome	Elongation factor Ts, mitochondrial	TSFM	143	39169	52	2.2	0.1	0.022
Qproteome	Protein FAM171B	FAM171B	61	100849	49	1.4	0.04	0.022
Qproteome	Kininogen-1	KNG1	1267	80489	48	20.3	0.72	0.326
Qproteome	WD repeat-containing protein 19	WDR19	47	166391	38	0.4	0.02	0.018
Qproteome	Plasminogen	PLG	521	100452	34	5.1	0.2	0.112
Qproteome	Beta-2-glycoprotein 1	APOH	282	44051	27	7.8	0.28	0.069
Qproteome	Serum amyloid P-component	APCS	780	27358	22	14.3	0.68	0.104
Qproteome	Transmembrane protein 201	TMEM201	42	76326	20	1.2	0.05	0.021
Qproteome	Complement C5	C5	504	207189	16	3.7	0.11	0.127
Qproteome	Complement component C6	C6	663	118022	16	6.7	0.13	0.085
Qproteome	Dynein heavy chain 8, axonemal	DNAH8	59	565682	16	0.3	0.01	0.032
Qproteome	Negative elongation factor B	COBRA1	87	71759	16	2.2	0.05	0.020
Qproteome	Inner centromere protein	INCENP	42	117004	16	2.7	0.03	0.020
Qproteome	Formin-like protein 1	FMNL1	32	132291	12	0.6	0.03	0.023
Qproteome	Vacuolar protein-sorting-associated protein 36	VPS36	40	48397	12	1.6	0.08	0.022
Qproteome	Actin, cytoplasmic 1	ACTB	474	44934	11	15.5	0.49	0.125
Qproteome	Pericentrin	PCNT	48	411049	11	0.5	0.01	0.023

Immuno-depletion method	Title	Gene Symbol	prot_score	prot_mass	prot_matches	prot_cover	emPAI	Average mg/mL in depleted plasma
Qproteome	Complement component C8 beta chain	C8B	462	73758	10	7.1	0.22	0.090
Qproteome	Tumor necrosis factor receptor superfamily member 8	TNFRSF8	86	69388	10	1	0.05	0.019
Qproteome	Staphylococcal nuclease domain-containing protein 1	SND1	45	111120	9	2.3	0.07	0.044
Qproteome	SET domain-containing protein 3	SETD3	37	73898	9	0.8	0.05	0.021
Qproteome	CAP-Gly domain-containing linker protein 1	CLIP1	29	183824	9	1	0.02	0.021
Qproteome	Retinol-binding protein 4	RBP4	349	25067	8	19.4	0.53	0.075
Qproteome	Alpha-2-antiplasmin	SERPINF2	396	57755	8	6.5	0.21	0.068
Qproteome	Heparanase	HPSE	46	67043	8	2.4	0.06	0.023
Qproteome	Actin-binding LIM protein 1	ABLIM1	32	97150	7	2.6	0.08	0.043
Qproteome	Trichoplein keratin filament-binding protein	TCHP	69	67056	7	2.8	0.06	0.023
Qproteome	Uncharacterized protein FLJ44048	-	59	205325	7	1.1	0.02	0.023
Qproteome	ADAMTS-like protein 1	ADAMTSL1	29	64754	7	0.4	0.06	0.022
Qproteome	P protein	OCA2	46	96527	7	0.7	0.04	0.022
Qproteome	Kappa-actin	FKSG30	65	45645	6	5.5	0.17	0.044
Qproteome	Probable E3 ubiquitin-protein ligase HECTD3	HECTD3	35	104187	6	1.4	0.04	0.023
Qproteome	Cyclin-dependent kinase-like 1	CDKL1	39	46856	6	2	0.08	0.020
Qproteome	Golgi resident protein GCP60	ACBD3	40	65308	6	1.3	0.06	0.020
Qproteome	ANKRD26-like family C member 1A	A26C1A	161	135563	5	2.6	0.08	0.061
Qproteome	Plasma kallikrein	KLKB1	97	79485	5	1.7	0.05	0.022
Qproteome	Zinc finger protein 37A	ZNF37A	47	74724	5	1.4	0.05	0.021
Qproteome	26S proteasome non-ATPase regulatory subunit 5	PSMD5	40	59730	5	1.4	0.06	0.020
Qproteome	Ras GTPase-activating protein SynGAP	SYNGAP1	33	158671	5	0.6	0.02	0.017
Qproteome	N-acetylmuramoyl-L-alanine amidase	PGLYRP2	161	64621	4	8	0.18	0.065
Qproteome	MAP7 domain-containing protein 1	MAP7D1	42	102617	4	1.5	0.04	0.022
Qproteome	Ladybird homeobox corepressor 1-like protein	CORL2	44	111363	4	0.8	0.03	0.019
Qproteome	Eukaryotic translation initiation factor 3 subunit J	EIF3J	29	34779	4	3.1	0.11	0.021
Qproteome	Syntaxin-1B	STX1B	41	37343	4	2.1	0.1	0.021

Immuno-depletion method	Title	Gene Symbol	prot_score	prot_mass	prot_matches	prot_cover	emPAI	Average mg/mL in depleted plasma
Qproteome	UDP-N-acetylglucosamine--peptide N-acetylglucosaminyltransferase 110 kDa subunit	OGT	47	125886	4	0.6	0.03	0.021
Qproteome	Envoplakin	EVPL	38	252963	4	0.4	0.01	0.014
Qproteome	Complement factor H-related protein 1	CFHR1	115	41216	3	6.7	0.19	0.043
Qproteome	DENN domain-containing protein 4C	DENND4C	50	204270	3	0.7	0.02	0.023
Qproteome	Disks large homolog 5	DLG5	36	233891	3	0.7	0.02	0.026
Qproteome	Putative myosin-XVB	MYO15B	47	176166	3	0.5	0.02	0.020
Qproteome	1-phosphatidylinositol-4,5-bisphosphate phosphodiesterase gamma-1	PLCG1	42	160269	3	0.5	0.02	0.018
Qproteome	Lebercilin-like protein	LCA5L	49	88817	2	1.3	0.04	0.020
Qproteome	FACT complex subunit SPT16	SUPT16H	28	135972	2	0.7	0.03	0.023
Qproteome	Complement component C8 gamma chain	C8G	120	23299	2	7.4	0.16	0.021
Qproteome	Complement component C8 alpha chain	C8A	75	71587	2	1.4	0.05	0.020
Qproteome	Structural maintenance of chromosomes protein 1B	SMC1B	32	165103	2	0.7	0.02	0.018
Qproteome	Platelet-activating factor acetylhydrolase	PLA2G7	44	54825	2	2.3	0.07	0.021
Qproteome	Tubulin polyglutamylase TTLL5	TTLL5	41	155257	2	0.5	0.02	0.017

J Proteome Res. Author manuscript; available in PMC 2013 December 07.

Table 4

Putative Concentrations of the Composite 412 Protein Plasma Proteome less Albumin and Immunoglobulins

Immuno-depletion method	Title	Gene Symbol	prot_score	prot_mass	prot_matches	prot_cover	emPAI	Average mg/mL in depleted plasma
Qproteome	Centrosomal protein of 164 kDa	CEP164	94	179858	78	0.4	0.02	0.020
Seppro	Attractin	ATRN	803	172529	48	5.8	0.21	0.020
Qproteome	Inner centromere protein	INCENP	42	117004	16	2.7	0.03	0.020
Qproteome	Tumor necrosis factor receptor superfamily member 8	TNFRSF8	86	69388	10	1	0.05	0.019
Seppro	Thrombospondin-1	THBS1	774	141361	23	7.1	0.23	0.017
Qproteome	Ras GTPase-activating protein SynGAP	SYNGAP1	33	158671	5	0.6	0.02	0.017
Seppro	Multiple epidermal growth factor-like domains protein 8	MEGF8	282	320217	10	3.2	0.07	0.012
Seppro	Neural cell adhesion molecule L1-like protein	CHL1	246	147296	28	2.4	0.13	0.010
Seppro	Phosphatidylcholine-sterol acyltransferase	LCAT	288	51762	11	5	0.32	0.009
Seppro	Pantetheinase	VNN1	295	60742	8	11.5	0.27	0.009
Seppro	Intercellular adhesion molecule 1	ICAM1	693	62046	17	8.8	0.26	0.009
Seppro	GDH/6PGL endoplasmic bifunctional protein	H6PD	118	93441	7	5.4	0.17	0.009
Seppro	Transforming growth factor-beta-induced protein ig-h3	TGFBI	808	80161	23	9.4	0.2	0.009
Seppro	Interleukin-1 receptor accessory protein	IL1RAP	269	72170	12	5.8	0.22	0.008
Seppro	Receptor-type tyrosine-protein phosphatase eta	PTPRJ	421	156271	9	4.6	0.1	0.008
Seppro	Nidogen-1	NID1	71	143465	4	2.6	0.11	0.008
Seppro	Neogenin	NEO1	147	170601	8	3.3	0.09	0.008
Seppro	Laminin subunit alpha-2	LAMA2	89	379925	22	2.1	0.04	0.008
Seppro	Tenascin-X	TNXB	306	488484	13	1.9	0.03	0.008
Seppro	1 Macrophage mannose receptor 1-like protein	MRC1L1	100	183170	4	3	0.08	0.008
Seppro	Platelet basic protein	PPBP	686	16188	22	18.8	0.91	0.008
Seppro	Intercellular adhesion molecule 2	ICAM2	345	32877	9	9.5	0.39	0.007
Seppro	Cell surface glycoprotein MUC18	MCAM	108	77287	19	2.8	0.15	0.006
Seppro	Hypoxia up-regulated protein 1	HYOU1	392	122734	13	6	0.09	0.006
Seppro	Vascular endothelial growth factor receptor 3	FLT4	184	155572	7	4.3	0.07	0.006

Immuno-depletion method	Title	Gene Symbol	prot_score	prot_mass	prot_matches	prot_cover	emPAI	Average mg/mL in depleted plasma
Seppro	Protein S100-A9	S100A9	110	15020	4	24.6	0.59	0.005
Seppro	Cystatin-C	CST3	379	17170	10	18.5	0.5	0.005
Seppro	Coiled-coil domain-containing protein 126	CCDC126	303	17244	8	8.6	0.5	0.005
Seppro	Centromere protein F	CENPF	36	417533	22	1	0.02	0.005
Seppro	Metalloproteinase inhibitor 1	TIMP1	281	25137	6	5.8	0.33	0.004
Seppro	C-reactive protein	CRP	289	27355	11	11.2	0.3	0.004
Seppro	Multimerin-2	MMRN2	195	110792	8	1.8	0.07	0.004
Seppro	Ficolin-2	FCN2	147	36885	8	6.7	0.21	0.004
Seppro	Noelin	OLFM1	177	59540	8	4.7	0.13	0.004
Seppro	L-selectin	SELL	108	47532	9	7	0.16	0.004
Seppro	Endoglin	ENG	255	74730	10	5.8	0.1	0.004
Seppro	Scavenger receptor cysteine-rich type 1protein M130	CD163	246	136636	9	2.1	0.05	0.004
Seppro	Plectin-1	PLEC1	40	569055	21	1.1	0.01	0.003
Seppro	Poly [ADP-ribose] polymerase 14	PARP14	54	218539	12	0.8	0.02	0.002
Seppro	Rapamycin-insensitive companion of mTOR	RICTOR	63	208185	22	1.2	0.02	0.002
Seppro	Phosphatidylinositol-4,5-bisphosphate 3-kinase catalytic subunit beta isoform	PIK3CB	74	135868	25	0.7	0.03	0.002
Seppro	Nucleoporin NUP188 homolog	NUP188	37	209465	8	0.3	0.02	0.002
Seppro	Pleckstrin homology domain-containing family A member 7	PLEKHA7	38	135984	22	1.2	0.03	0.002
Seppro	Enhancer of polycomb homolog 1	EPC1	47	102045	69	1.8	0.04	0.002
Seppro	Kinesin-like protein KIF21B	KIF21B	104	199879	49	1	0.02	0.002
Seppro	Atrophin-1	ATN1	40	130632	28	1	0.03	0.002
Seppro	MIF4G domain-containing protein	MIF4GD	67	27334	18	2.7	0.14	0.002
Seppro	Formin-2	FMN2	36	194304	12	0.6	0.02	0.002
Seppro	Probable ATP-dependent RNA helicase DDX41	DDX41	44	77826	5	1.1	0.05	0.002
Seppro	Uncharacterized protein C2orf77	C2orf77	100	77323	22	1.1	0.05	0.002
Seppro	Probable G-protein coupled receptor 25	GPR25	46	39984	5	1.9	0.09	0.002
Seppro	Tumor necrosis factor receptor superfamily member 10A	TNFRSF10A	37	53964	12	1.5	0.07	0.002

Immuno-depletion method	Title	Gene Symbol	prot_score	prot_mass	prot_matches	prot_cover	emPAI	Average mg/mL in depleted plasma
Seppro	Interleukin-12 receptor subunit beta-1	IL12RB1	36	77456	12	0.9	0.05	0.002
Seppro	Plexin domain-containing protein 2	PLXDC2	153	62998	5	2.1	0.06	0.002
Seppro	SPRY domain-containing protein 3	SPRYD3	34	53346	6	1.4	0.07	0.002
Seppro	HMG domain-containing protein 3	HMGXB3	62	181488	9	0.5	0.02	0.002
Seppro	Calcyclin-binding protein	CACYBP	108	31207	43	5.7	0.12	0.002
Seppro	UPF0505 protein C16orf62	C16orf62	82	120515	4	2.1	0.03	0.002
Seppro	Synaptotagmin-13	SYT13	46	51806	15	2.6	0.07	0.002
Seppro	Cholesteryl ester transfer protein	CETP	169	59011	4	3	0.06	0.002
Seppro	ATP-binding cassette sub-family B member 9	ABCB9	232	88768	17	0.9	0.04	0.002
Seppro	E3 ubiquitin-protein ligase TRIM37	TRIM37	70	116552	6	1.7	0.03	0.002
Seppro	26S proteasome non-ATPase regulatory subunit 1	PSMD1	38	117026	8	1	0.03	0.002
Seppro	Sodium- and chloride-dependent transporter XTRP3	SLC6A20	37	69839	7	1	0.05	0.002
Seppro	Retina-specific copper amine oxidase	AOC2	38	86239	6	0.8	0.04	0.002
Seppro	DNA ligase 1	LIG1	31	112676	6	1.2	0.03	0.002
Seppro	Leucine-rich repeat serine/threonine-protein kinase 2	LRRK2	36	315074	4	0.4	0.01	0.002
Seppro	Structural maintenance of chromosomes protein 3	SMC3	35	160154	23	2.2	0.02	0.002
Seppro	Cohesin subunit SA-1	STAG1	54	156257	10	1	0.02	0.002
Seppro	Centrosomal protein of 135 kDa	CEP135	34	149283	17	1	0.02	0.002
Seppro	Voltage-dependent N-type calcium channel subunit alpha-1B	CACNA1B	56	279251	22	0.6	0.01	0.001
Seppro	Nuclear mitotic apparatus protein 1	NUMA1	104	261102	21	0.7	0.01	0.001